Journal of Applied Electrochemistry **31**: 1149–1153, 2001.

Synthesis and electrochemical characterization of a new Se-doped spinel material for lithium secondary batteries

Y-K. SUN*
Department of Chemical Engineering, Hanyang University, Sungdong-Gu, Seoul, 133-791, Korea
*(*author for correspondence)*

Received 11 January 2001; accepted in revised form 5 June 2001

Key words: Jahn–Teller distortion, lithium manganese oxide, lithium secondary batteries, Se-doped spinel, sol–gel method

Abstract

A new Se-doped spinel material, $LiAl_{0.18}Se_{0.02}Mn_{1.8}O_4$ powder with a phase-pure polycrystalline was synthesized by a sol–gel method. The material in the 3 V region (2.4 $\sim$ 3.5 V) and both the 3 and 4 V region (2.4 $\sim$ 4.4 V) initially deliver a discharge capacity of 81 and 178 mA h g^{-1} which increase with cycling to reach 110 and 204 after 50 cycles, respectively. The material shows excellent cycleability in the 4 V region (3.0 $\sim$ 4.4 V) with almost no capacity loss. The structural integrity of the Se-doped spinel was characterized by charge–discharge cycling tests and X-ray diffraction.

1. Introduction

Spinel $LiMn_2O_4$ and its derivatives have generated great interest as promising cathode materials (positive electrodes) for lithium secondary batteries due to their low cost, abundance, and nontoxicity compared with the layered oxides such as $LiCoO_2$ and $LiNiO_2$ [1–4]. However, a capacity loss of the spinel $LiMn_2O_4$ during cycling prevents its wider use as cathode material for lithium secondary batteries [5–8], especially in the 3 V region.

$Li_xMn_2O_4$ $(x = 1)$ has a cubic spinel structure with space group symmetry Fd3m in which lithium ions are located at the 8a tetrahedral sites and the manganese ions at the 16d octahedral sites of the cubic unit cell. In $Li/Li_xMn_2O_4$ cells, when $0 \leqslant x \leqslant 1$, the cell discharges at 4 V (4 V region) vs Li/Li^+, whereas when $1 \leqslant x \leqslant 2$, the cell discharges at 3 V (3 V region) vs Li/Li^+ [9, 10]. Although the unit cell contracts and expands by 7.6%, it does so gradually and isotropically so that the cubic symmetry of the spinel $Li_xMn_2O_4$ is maintained while Li^+ ions is reversibly inserted into 8a tetrahedral sites in the 4 V region [9, 10]. However, capacity still slowly fades during cycling in this voltage region. The main cause of the capacity loss in the 4 V region has been reported to be the solubility of the spinel electrode in the electrolyte due to the formation of HF resulting from reaction of fluorinated anions with residual H_2O [11–13]. Recently, we reported that the formation of rock salt Li_2MnO_3 at the surface of a spinel electrode was responsible for the structural degradation of the spinel host which, in turn, resulted in capacity loss in the 4 V region [14]. To date, efforts have been made to improve the 4 V cycleability, and some of these efforts have been successful in improving the cycleability in the $Li/Li_xMn_2O_4$ cell in the 4 V region [15–19]. However, there have been few reports on stabilizing the Jahn–Teller distortion in the 3 V region, and no research groups have overcome the Jahn–Teller distortion in the spinel $LiMn_2O_4$ phase [6, 20, 21].

Recently, the author reported that sulfur-doped spinel materials synthesized by a sol–gel method such as $LiAl_{0.24}Mn_{1.76}O_{3.98}S_{0.02}$, $Li_{1.02}Al_{0.25}Mn_{1.75}O_{3.97}S_{0.03}$, and $Li_{1.03}Al_{0.2}Mn_{1.8}O_{3.96}S_{0.04}$, showed excellent cycleability in the 3 V region as well as the 4 V region, which was ascribed to the effects of Al and S substitution for Mn and O in the spinel $LiMn_2O_4$ host, respectively [19, 22–24].

Here we synthesize a new Se-doped spinel material, $LiAl_{0.18}Se_{0.02}Mn_{1.8}O_4$ using a sol–gel method and evaluate its electrochemical performance. The structure of $LiAl_{0.18}Se_{0.02}Mn_{1.8}O_4$ powders was investigated before and after charge–discharge cycling. The charge–discharge behaviour was evaluated in the operating voltage ranges 3.0–4.4 V (4 V region) and 2.4–3.5 V (3 V region), and 2.4–4.4 V (both the 3 and 4 V region) (vs Li/Li^+). The electrochemical and structural characteristics of $LiAl_{0.2}Mn_{1.8}O_4$ compared with $LiAl_{0.18}Se_{0.02}Mn_{1.8}O_4$ spinel are also discussed.

2. Experimental details

$LiAl_{0.18}Se_{0.02}Mn_{1.8}O_4$ powders were prepared by a sol–gel method using glycolic acid as a chelating agent

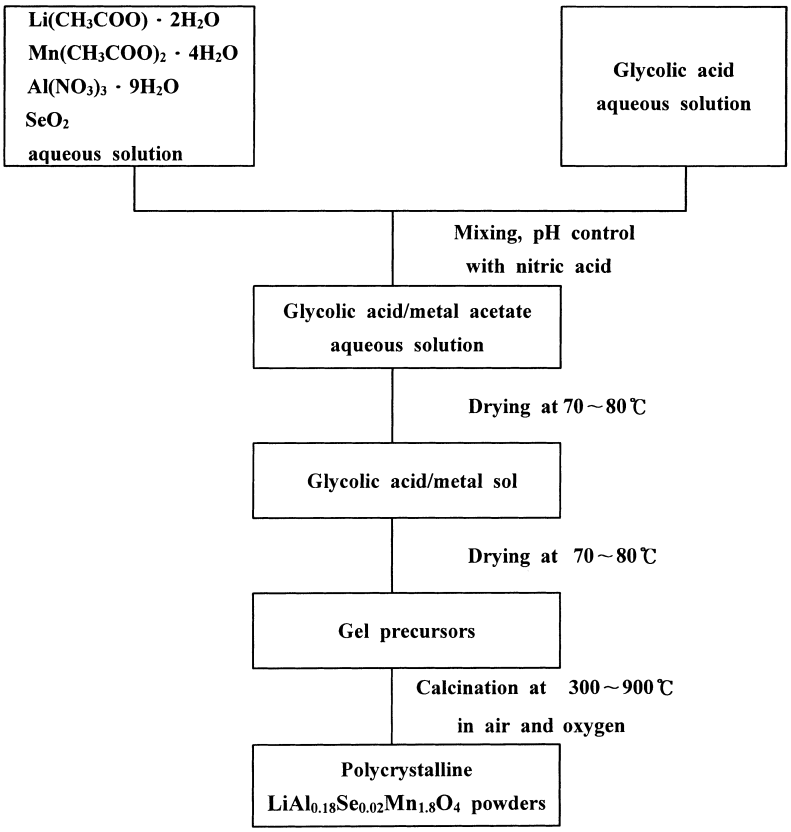

Fig. 1. Flowsheet of the procedure preparing polycrystalline $LiAl_{0.18}$ $Se_{0.02}Mn_{1.8}O_4$ powders by a sol–gel method.

according to the procedure shown in Figure 1. $LiAl_{0.18}$ $Se_{0.02}Mn_{1.8}O_4$ is the composition for calculating the ratio of starting material. $Li(CH_3COO) \cdot 2H_2O$ (Kanto Chemical Co.), $Mn(CH_3COO)_2 \cdot 4H_2O$ (Acros Organics), $Al(NO_3)_3 \cdot 9H_2O$ (Aldrich Chemical Co.), and SeO_2 (AldrichChemical Co.) (cationic ratio of Li:Mn:Al:Se = 1.06:1.8:0.18:0.2) were dissolved in distilled water, and added dropwise to a continuously stirred aqueous solution of glycolic acid (Kanto Chemical Co.). The pH of the solution was adjusted to $3 \sim 4$ using nitric acid. The resultant solution was evaporated at $70 \sim 80$ °C until a transparent sol and gel was obtained. The resulting gel precursors were decomposed at 500 °C for 10 h in air, calcined at 800 °C in air for 10 h, and then in flowing oxygen for 12 h. For the preparation of $LiAl_{0.2}Mn_{1.8}O_4$ powders, the same procedure with different cationic molar ratio ($Li(CH_3COO) \cdot H_2O$:$Al(NO_3)_3 \cdot 9H_2O$:$Mn(CH_3COO)_2 \cdot 4H_2O$ = 1.06:0.2:1.8) was repeated.

Powder X-ray diffraction (Rigaku, Rint-2000) using CuK_α radiation was used to identify the crystalline phase of the as-prepared powders and cycled electrodes. Rietveld refinement was then performed on the X-ray diffraction data to obtain lattice constants. The contents of lithium, aluminum, selenium and manganese were measured with an inductively coupled plasma (ICP) by dissolving the powders in dilute nitric acid.

Electrochemical properties of the Se-doped spinel, $LiAl_{0.18}Se_{0.02}Mn_{1.8}O_4$ were evaluated with a two-electrode cells using the spinel electrode, a Li metal anode, a microporous separator and an electrolyte (Cheil Industries Inc., battery grade) consisting of a 1:1 mixture of ethylene carbonate (EC) and propylene carbonate (PC) containing 1 M $LiClO_4$ by volume. The cathode was fabricated by mixing the $LiAl_{0.18}Se_{0.02}Mn_{1.8}O_4$ powders with 12 wt % of carbon black and 8 wt % of polytetrafluoroethylene (PTFE), the mixture was pressed onto aluminum Exmet, and then dried in a vacuum at 120 °C for 12 h. The charge–discharge cycle was performed galvanostatically at a current density of 0.2 mA cm^{-2} at room temperature.

3. Results and discussion

The chemical analysis data show the $Li_{1.06}Al_{0.18}Se_{0.2}$-$Mn_{1.8}O_4$ and $Li_{1.06}Al_{0.2}Mn_{1.8}O_4$ to be $LiAl_{0.18}Se_{0.02}$-$Mn_{1.8}O_4$ and $LiAl_{0.2}Mn_{1.8}O_4$, respectively. Figure 2 shows X-ray diffraction (XRD) patterns of $LiAl_{0.18}$-$Se_{0.02}Mn_{1.8}O_4$ (Figure 2(a)) and $LiAl_{0.2}Mn_{1.8}O_4$ (Figure 2(b)). It is observed that the two spinel powders are confirmed to be the well-defined spinel phase with space group *Fd3m*. The lattice constant (*a*) of the $LiAl_{0.18}$-$Se_{0.02}Mn_{1.8}O_4$ and $LiAl_{0.2}Mn_{1.8}O_4$ powders are 8.195 and 8.1775 Å, respectively which are much lower than that of stoichiometric spinel [10, 11]. It is reported that the lattice constant of metal-doped $LiM_xMn_{2-x}O_4$ spinel structures decreases with increasing the amount of doped metal due to an increasing concentration of

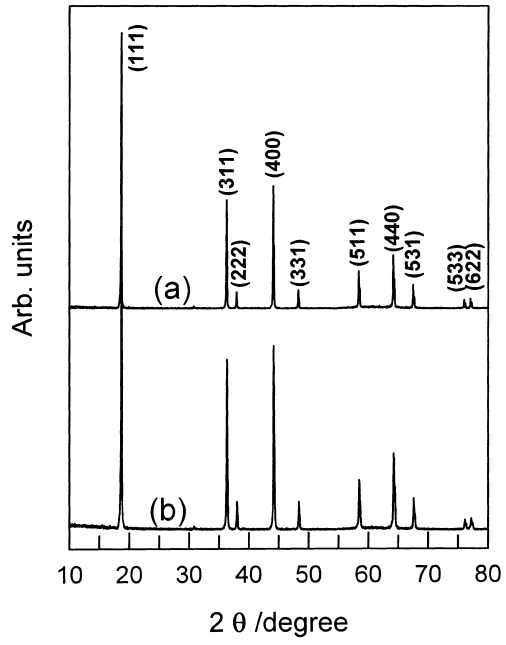

Fig. 2. X-ray diffraction patterns of the $LiAl_{0.18}Se_{0.02}Mn_{1.8}O_4$ and $LiAl_{0.2}Mn_{1.8}O_4$ powders.

Mn^{4+} ions in the spinel structure [17], which increases cycleability in the 4 V region.

Figure 3 represents the charge–discharge curves in three different voltage ranges (4.4 $\sim$ 3.0 V, 2.4 $\sim$ 3.5 V, and 2.4 $\sim$ 4.4 V) as a function of cycle number at a constant current density of 0.2 mA cm^{-2} in room temperature. The $Li/LiAl_{0.18}Se_{0.02}Mn_{1.8}O_4$ cell in the 4 V region exhibits only one plateau, delivers an initial capacity of 111 mA h g^{-1}, and shows excellent capacity retention with very low capacity decrease. The capacity loss in this voltage region could be ascribed to the appearance of rock salt Li_2MnO_3 phase at the surface of the spinel electrode resulting from MnO dissolution via the disproportionation reaction ($Li_2Mn_2O_4 \rightarrow Li_2MnO_3 +$ MnO) though a small amount of Li_2MnO_3 was not detected in the XRD patterns [14]. The electrochemical cycleability of the $LiAl_{0.18}Se_{0.02}Mn_{1.8}O_4$ electrode was examined in the 3 V region cycled between 3.5 and 2.4 V since spinel $LiMn_2O_4$ loses capacity in this voltage region due to the Jahn–Teller distortion. It is interesting to see that the $Li/LiAl_{0.18}Se_{0.02}Mn_{1.8}O_4$ cell initially delivers a discharge capacity of 81 mA h g^{-1} gradually increases with cycling to reach 110 mA h g^{-1} after 50 cycles as shown in Figure 2(b). This unusual cycling behavior, similar to the S-doped spinel materials, is unique feature, different from those of the spinel $LiMn_2O_4$ and its derivatives [20, 21, 25]. It is well known that spinel suffers from severe capacity loss in the 3 V region. The voltage plateau occurring at about 2.85 V is mainly due to the intercalation of Li^+ ions into cubic $LiMn_2O_4$ to form tetragonal $Li_2Mn_2O_4$ [5, 9, 10]. This structural distortion cause the 16% increase in the c/a ratio, and the imposed volume change is too great for the individual spinel particles to maintain structural integrity, thereby resulting in a rapid capacity loss [9, 10]. Although a small

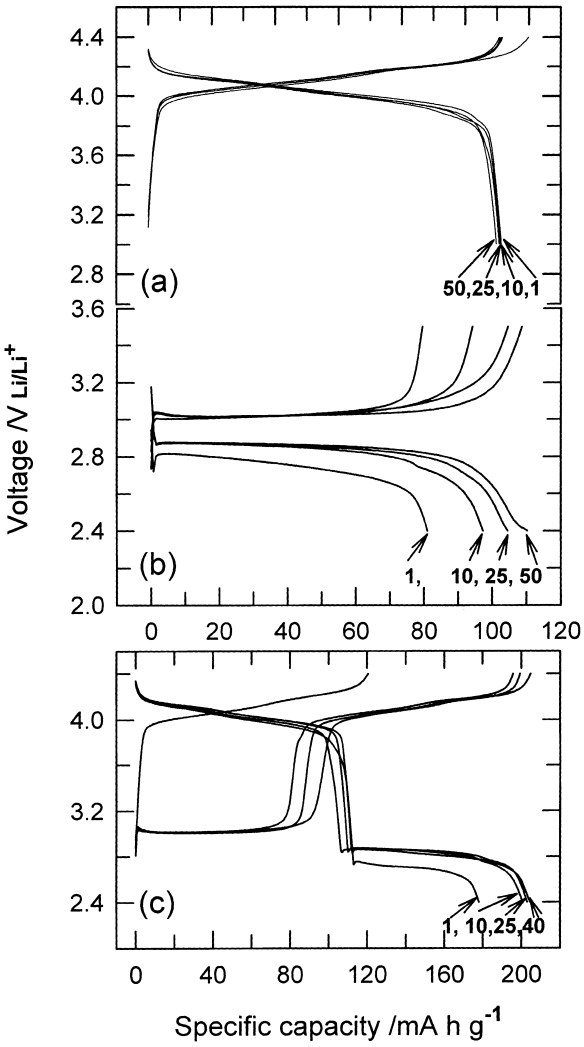

Fig. 3. Cycling charge–discharge curves for $Li/LiAl_{0.18}Se_{0.02}Mn_{1.8}O_4$ cell in the voltage range of (a) 4.4–3.0, (b) 2.4–3.5, (c) and 2.4–4.4 V.

amounts of Se and S was detected in the Se-doped and S-doped spinel materials, respectively, the Se and S ions in the spinel structure play an important role in the unusual cycling behaviour in the 3 V region [19, 24]. It is speculated that this behavior may be due to the rearrangement of Li^+ ions by intercalating the empty 16c octahedral sites in the $LiAl_{0.18}Se_{0.02}Mn_{1.8}O_4$ host structure during cycling. At this point, it is not clear why the capacity in the 3 V region increases with the cycle number. Shown in Figure 3(c) are the charge–discharge curves of the material in the voltage range of 2.4 $\sim$ 4.4 V. Whereas the discharge capacity in the 4 V region remains almost constant, that in the 3 V region increases rapidly up to 10 cycles and subsequently stabilizes on further cycling. The $LiAl_{0.18}Se_{0.02}Mn_{1.8}O_4$ electrode initially delivers capacity of 178 mA h g^{-1} and reaches to 204 mA h g^{-1} after 25 cycles. Although the Se-doped spinel material exhibits a larger voltage drop between the 4 and 3 V plateaus, it delivers a large capacity with excellent cycleability, and therefore it could be used as a promising cathode material for lithium secondary batteries.

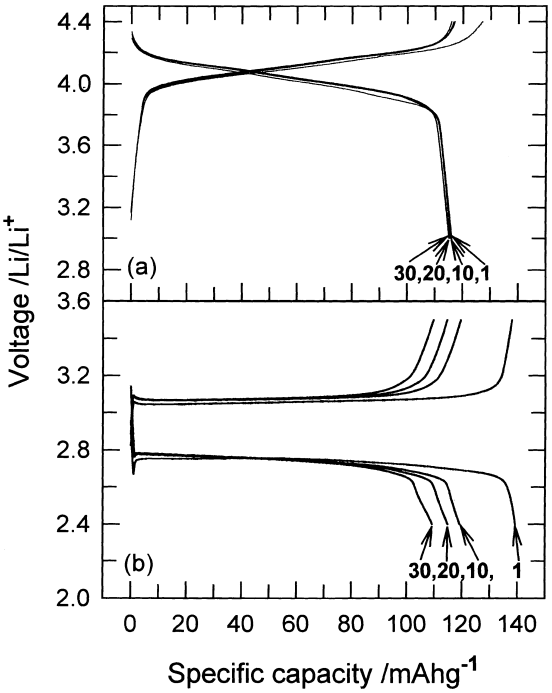

Fig. 4. Cycling charge–discharge curves for $Li/LiAl_{0.2}Mn_{1.8}O_4$ cell in the voltage range of (a) 4.4–3.0 and (b) 2.4–3.5 V.

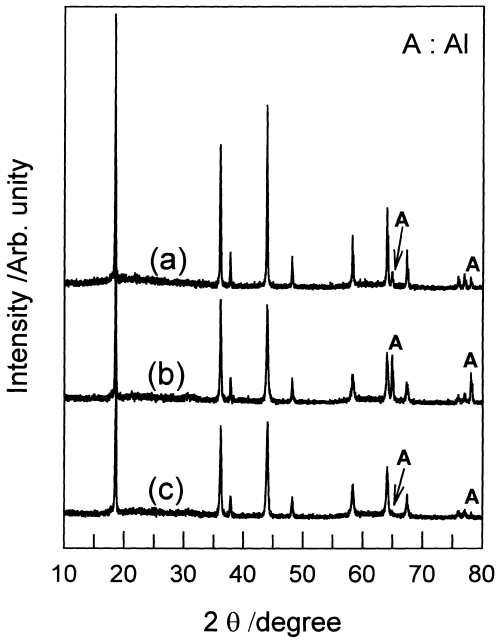

Fig. 5. X-ray diffraction patterns for the cycled $LiAl_{0.18}Se_{0.02}Mn_{1.8}O_4$ electrodes after 50 cycles in the voltage range of (a) 4.4–3.0, (b) 2.4–3.5, and (c) 4.4–2.4 V.

To compare the electrochemical properties of the Se-doped spinel, $LiAl_{0.18}Se_{0.02}Mn_{1.8}O_4$ with that of $LiAl_{0.2}Mn_{1.8}O_4$ spinel, we measured the charge–discharge behavior of $LiAl_{0.2}Mn_{1.8}O_4$ spinel in the 4 and 3 V region and the results are shown in Figure 4. The $LiAl_{0.2}Mn_{1.8}O_4$ electrode in the 4 V region delivers an initial discharge capacity of 115 mA h g^{-1} without any capacity loss up to the 30th cycle. On the other hand, the discharge capacity in the 3 V region rapidly decreases from 139 to 119 mA h g^{-1} within the first 10 cycles and then steadily decreases on further cycling. At the 30th cycle the electrode delivers 109 mA h g^{-1} which is 78% of the initial capacity of 139 mA h g^{-1}. The cycling behavior of the $LiAl_{0.2}Mn_{1.8}O_4$ electrode in the 4 and 3 V region is similar to the stoichiometric and its derivatives [10]. These results imply that the substitution Se for Mn is very effective improving the cycleability in the 3 V region.

It is believed that the excellent cycleability of the Se-doped spinel, $LiAl_{0.18}Se_{0.02}Mn_{1.8}O_4$ in the 3 V, 4 V, both 3 and 4 V region may be associated with to the structural stability of the host structure. To understand possible structural stability of the unusual cycling behavior of the material, the electrodes obtained from the material shown in Figure 3 were characterized by XRD. Figure 5 shows the XRD patterns for the electrodes after 50 cycles in the 4 V, 3 V, and both 3 and 4 V regions. The $LiAl_{0.18}Se_{0.02}Mn_{1.8}O_4$ electrode was allowed to equilibrate for 5 h at fully discharged state (2.4 and 3.0 V in the 3 V and the 4 V region, respectively) and then the electrode was dried for 1 day after removal from the cell in a glove box. When comparing XRD patterns for the cycled electrodes at various voltage ranges (Figure 5(a)–(c)) with that of as-prepared powders (Figure 2(a)), we are unable to find any difference in the positions of the characteristic peaks for the typical spinel phase. Although there are some variation of the peak intensities, no tetragonal phases were appeared. This result indicates that the electrode structure retains its original cubic spinel phase even after cycling in the 3 V region. This sort of XRD data was observed in the previously reported papers in which $LiAl_{0.24}Mn_{1.76}O_{3.98}S_{0.02}$ electrode was cycled in the 3 V region [19, 22–24].

Figure 6 shows the XRD patterns for the $LiAl_{0.2}Mn_{1.8}O_4$ electrodes after 30 cycles in the 3 and 4 V region. The sample for the XRD analysis were prepared in the same way described above. For the $LiAl_{0.2}Mn_{1.8}O_4$ electrode cycled in the 4 V region, the XRD patterns exhibits typical characteristic peaks for the spinel structure compared with the as-prepared powders (Figure 2(b)). As shown in Figure 6(b), however, the XRD patterns for the $LiAl_{0.2}Mn_{1.8}O_4$ electrode cycled in the 3 V region, showing serious capacity loss in Figure 4(b), exhibits the emergence of peaks relating to tetragonal $Li_2Mn_2O_4$ phase due to the occurrence of Jahn–Teller distortion. Similar results already reported in $LiAl_{0.24}Mn_{1.76}O_4$ electrode cycled in the 3 V region [22, 24]. Therefore, it is concluded that the excellent cycleability of $LiAl_{0.18}Se_{0.02}Mn_{1.8}O_4$ electrode in the 3 and 4 V region is due to the substitution Se and Al for Mn, respectively. The preservation of the cubic spinel phase of the cycled electrodes results in the enhancement of the electrochemical cycleability during cycling. This result encourages us to believe that the $LiAl_{0.18}Se_{0.02}Mn_{1.8}O_4$ could overcome the Jahn–Teller distortion.

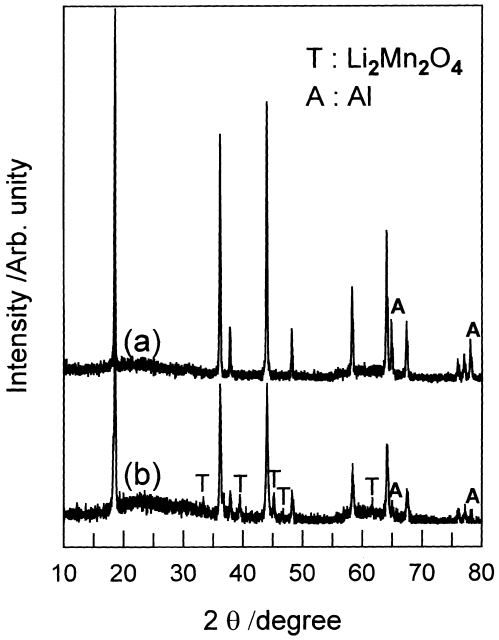

Fig. 6. X-ray diffraction patterns for the cycled $LiAl_{0.2}Mn_{1.8}O_4$ electrodes after 50 cycles in the voltage range of (a) 4.4–3.0 and (b) 2.4–3.5 V.

At this stage, though it is hard to explain why the Se-doped spinel $LiAl_{0.18}Se_{0.02}Mn_{1.8}O_4$ exhibits no capacity loss in the 3 V region, the substitution of Se for Mn is very effective in impeding the formation of tetragonal $Li_2Mn_2O_4$ structure on the $LiMn_2O_4$ host in the lower voltage range [19, 22–24]. To explore no capacity-loss phenomena in the 3 V region, more systematic experiments and characterization are under way.

4. Conclusion

A new Se-doped spinel, $LiAl_{0.18}Se_{0.02}Mn_{1.8}O_4$ was synthesized by a sol–gel method using glycolic acid as a chelating agent. The $LiAl_{0.18}Se_{0.02}Mn_{1.8}O_4$ electrode shows excellent cycleability with no capacity loss in the 4 V region and the discharge capacity of the electrode during cycling increases in the 3 V region, both 3 and 4 V region. It exhibits capacities of 110, 100, and 204 mA h g^{-1} in the 4 V, 3 V, and both the 3 V and 4 V regions. XRD results show that the $LiAl_{0.18}Se_{0.02}Mn_{1.8}O_4$ electrodes after cycling retain their original cubic spinel structure at all the operating voltage regions. This result encourages us to believe that the Se-doped spinel overcomes the Jahn–Teller distortion. Further crystallographic study is necessary to clarify the reason why the material maintains its original structure even after 50 cycles in wide voltage ranges.

Acknowledgements

This work was supported in part by the Ministry of Information & Communication of Korea (Support Project of University Information Technology Research Center, supervised by IITA).

References

1. T. Ohuzuku, M. Kitagawa and T. Hirai, *J. Electrochem. Soc.* **137** (1990) 760.
2. W.J. Macklin, R.J. Neat and R.J. Powell, *J. Power Sources* **34** (1991) 39.
3. V. Manev, A. Momchilov, A. Nassalevska and A. Kozawa, *J. Power Sources* **41** (1993) 305.
4. D. Guyomard and J.M. Tarascon, *Solid State Ionics* **69** (1994) 222.
5. R.J. Gummow, A. de Kock and M.M. Thackeray, *Solid State Ionics* **69** (1994) 59.
6. P. Barboux, J.M. Tarascon and F.K. Shokoohi, *J. Solid State Chem.* **94** (1991) 185.
7. H. Huang and P.G. Bruce, *J. Power Sources* **54** (1995) 52.
8. P. Arora, B.N. Popov and R.E. White, *J. Electrochem. Soc.* **145** (1998) 807.
9. M.M. Thackeray, P.G. David, P.G. Bruce and J.B. Goodenough, *Mat. Res. Bull.* **18** (1983) 461.
10. M.M. Thackeray, *Prog. Solid State Chem.* **25** (1997) 1.
11. D.H. Jang, Y.J. Shin and S.M. Oh, *J. Electrochem. Soc.* **143** (1996) 2204.
12. D.H. Jang and S.M. Oh, *J. Electrochem. Soc.* **144** (1996) 3342.
13. G.G. Amatucci, C.N. Schmutz, A. Bylr, C. Sigala, A.S. Gozdz, D. Larcher and J.M. Tarascon, *J. Power Sources* **69** (1997) 11.
14. Y-K. Sun, G-S. Park, Y-S. Lee, M. Yoshio and K.S. Nahm, *J. Electrochem. Soc.* submitted.
15. G.G. Amatucci, A. Bylr, C. Schmutz and J.M. Tarascon, *Prog. Batt. Batt. Mat.* **16** (1997) 1.
16. G.G. Amatucci and J.M. Tarascon, *US Patent 5 674 645* (1997).
17. G.G. Amatucci, A. Bylr, C. Siagala, P. Alfonse and J.M. Tarascon, *Solid State Ionics* **104** (1997) 13.
18. Y-K. Sun, *Solid State Ionics* **100** (1997) 115.
19. Y-K. Sun, Y-S. Jeon and H.J. Lee, *Electrochem. & Solid-State Lett.* **3** (2000) 7.
20. J.M. Tarascon, E. Wang, F.K. Shokoohi, W.R. McKinnon and S. Colson, *J. Electrochem. Soc.* **138** (1991) 2859.
21. H. Huang and P.G. Bruce, *J. Power Sources* **54** (1995) 52.
22. Y-K. Sun and Y-S Jeon, *Electrochem. Commun.* **1** (1999) 597.
23. Y-K. Sun, Y-S. Jeon, *J. Mater Chem.* **9** (1999) 3147.
24. S.H. Park, K.S. Park, Y-K. Sun and K.S. Nahm, *J. Electrochem. Soc.* **147** (2000) 2116.
25. Z. Jiang and K.M. Abraham, *J. Electrochem. Soc.* **143** (1996) 1591.